HHS Public Access

Author manuscript

Proc SPIE Int Soc Opt Eng. Author manuscript; available in PMC 2015 September 24.

Published in final edited form as:

Proc SPIE Int Soc Opt Eng. 2015 ; 9419: . doi:10.1117/12.2082326.

3D *in vivo* imaging of rat hearts by high frequency ultrasound and its application in myofiber orientation wrapping

Xulei Qin[1], **Silun Wang**[2], **Ming Shen**[3], **Xiaodong Zhang**[2], **Stamatios Lerakis**[3,1], **Mary B. Wagner**[4], and **Baowei Fei**[1,5,*]

[1]Department of Radiology and Imaging Sciences, Emory University, Atlanta, GA

[2]Yerkes National Primate Research Center, Emory University, Atlanta, GA

[3]Division of Cardiology, Department of Medicine, Emory University, Atlanta, GA

[4]Department of Pediatrics, Emory University, Atlanta, GA

[5]Department of Biomedical Engineering, Emory University and Georgia Institute of Technology, Atlanta, GA

Abstract

Cardiac ultrasound plays an important role in the imaging of hearts in basic cardiovascular research and clinical examinations. 3D ultrasound imaging can provide the geometry or motion information of the heart. Especially, the wrapping of cardiac fiber orientations to the ultrasound volume could supply useful information on the stress distributions and electric action spreading. However, how to acquire 3D ultrasound volumes of the heart of small animals *in vivo* for cardiac fiber wrapping is still a challenging problem. In this study, we provide an approach to acquire 3D ultrasound volumes of the rat hearts *in vivo*. The comparison between both *in vivo* and *ex vivo* geometries indicated 90.1% Dice similarity. In this preliminary study, the evaluations of the cardiac fiber orientation wrapping errors were 24.7° for the acute angle error and were 22.4° for the inclination angle error. This 3D ultrasound imaging and fiber orientation estimation technique have potential applications in cardiac imaging.

Keywords

In vivo 3D ultrasound imaging; cardiac fiber orientations; magnetic resonance diffusion tensor imaging (MR-DTI); small animal imaging; cardiac imaging; echocardiography

1. INTRODUCTION

Ultrasound imaging plays an important role in cardiovascular research and clinical examinations [1, 2]. The acquisition of cardiac image volumes can provide 3D geometry and comprehensive motion information of the heart. Moreover, as cardiac fiber orientations affect the cardiac anatomy, mechanical properties, and the electrophysiology inside the heart [3–5], the wrapping of cardiac fiber orientations to the ultrasound volume can supply useful

*bfei@emory.edu; web: http://feilab.org.

information on stress distributions and electric action spreading. Currently, cardiac ultrasound imaging for the small animal hearts is generally in 2D, which only provides 2D images and requires geometric assumption for left ventricle calculations. It is still challenging to design a 3D ultrasound probe for small animal heart applications because of the high ultrasound frequency (>15 MHz).

For 3D ultrasound imaging of small animals, Dawson et al. developed a highly accurate, reconstructive 3D ultrasound imaging system for mouse hearts [6]. Further applications of 3D ultrasound imaging in small animal studies were summarized in [7]. However, there was no reliable method on 3D ultrasound imaging of rat hearts. In this study, we designed a 3D ultrasound volume acquisition approach for rat hearts *in vivo*. Especially for quantifying the right ventricular geometry or for the cases of severe heart remodeling, we tested the feasibility of *in vivo* imaging of a beating heart using an open-chest procedure. After image acquisition, the segmented cardiac myocardium is then reconstructed into 3D geometry.

For indirectly estimation of cardiac fiber orientation, the procedure of wrapping cardiac fiber orientations from DTI data of a template heart to the target heart has been applied to the MRI, CT and ultrasound modalities as reported by others and our group [5, 8, 9]. In this study, we further apply the procedure of mapping the cardiac fiber orientations to *in vivo* beating hearts. The accuracy of the cardiac fiber orientation wrapping method is quantitatively validated using magnetic resonance diffusion tensor imaging (MR-DTI). This is an important step to translate the ultrasound-based cardiac fiber estimation method from animals to humans.

2. METHODS

2.1 3D ultrasound imaging *in vivo*

The rat was settled on the imaging platform and was imaged by the Vevo 2100 ultrasound system (FUJIFILM VisualSonics, Inc., Toronto, Canada) with a 21 MHz transducer. B-mode ultrasound images of the hearts in the short-axis view were acquired slice by slice from base to apex at a 0.2 mm thickness. Each slice position was dynamically imaged as a serial of beating cycles. The pixel size in the B-mode image was 0.06 mm. During the image acquisition, both ECG and respiration signals were recorded. However, this method can have limitations in cases when the myocardial boundaries of the whole heart are required and when it is critical to accurately quantify the right ventricular geometry for severe heart remodeling. In order to image the 3D geometry of the remodeled geometry, the *in vivo* imaging procedure is performed on the beating heart after an open-chest surgical procedure. During imaging, the respiratory of the rat is kept by a respiratory machine and ECG signals are recorded.

2.2 Diffusion tensor imaging of rat hearts *ex vivo*

After *in vivo* ultrasound imaging, the rat heart was excised and then embedded in 2% agar phantoms for the MR imaging procedures. The phantoms were placed in a Biospec 7 T MRI system (Bruker Corporation, Massachusetts, USA). An RF coil with an inner diameter of 30 mm was used to transmit/receive the signals. Before diffusion tensor imaging, T1

anatomical images were acquired at a voxel resolution of 0.078 × 0.078 ×0.156 mm^3. Then, the cardiac fiber orientations were imaged in 30 directions using a spin echo sequence at the 0.234 mm isotropic resolution. Total MRI time was 36 hours for each heart.

2.3 Mapping cardiac fiber orientation from diffusion tensor imaging to 3D ultrasound

Geometry and fiber orientation reconstruction—After data acquisition, the both ultrasound and MR images are processed. First, the end of systolic volume was selected from the ultrasound sequences based on the ECG signals and respiration signals. Both the ultrasound images and T1-weighted MR images were manually segmented using the Analyze software (AnalyzeDirect Inc., Overland Park, KS). The binary geometric volumes of the hearts were reconstructed. Based on the segmented heart mask from T1-MR images, the cardiac fiber orientations were reconstructed from the DTI data.

Cardiac fiber orientation wrapping—For warping of the cardiac fiber orientation from MR-DTI data, the 3D ultrasound images are registered with the T1-MRI data. Various imaging registration methods were developed in our group [15–23]. In this procedure, there are two steps to wrap cardiac fiber orientations from DTI to the target ultrasound geometries, which is illustrated in Figure 1.

The first step is to generate the deformation field between the ultrasound geometry of the target heart and the MRI geometry of the template heart. During the geometry registration step, the atlas geometry is first registered to target geometry by supervised affine transformations (translation, rotation, shear, and scaling) using Analyze software. After that, a diffeomorphic Demons registration method was applied to perform a deformable registration. In order to match two images I_0 and I_1 by a transformation s, the typical Demons registration requires a similarity criterion $Sim(I_0, I_1, S)$ to measure the similarity between both images, and also a regularization energy $Reg(s)$ to evaluate their transformation likelihood. They are defined as follows:

$$E(s) = \frac{1}{\sigma_i^2} Sim(I_0, I_1, S) + \frac{1}{\sigma_T^2} Reg(S), \quad (1)$$

where σ_i relates to the noise of the image and σ_T weighs the regularization effect. However, traditional Demons registration methods usually cannot supply the diffeomorphic transformations which are necessary for maintaining the topology of the cardiac anatomical structures and the invertible deformation field for the fiber reorientations of DTI data. Thus, Vercauteren *et al.* adapted the Demons as an optimization procedure on the entire space of displacement fields to a space of diffeomorphic transformations through the exponential. The modified energy function is described as followed

$$E_{diffeo}(I_0, I_1, s, u) = Sim(I_0, I_1, s^{\circ} exp(u)) + \|u\|^2, \quad (2)$$

where u is the velocity field and $\|u\|$ is its norm. Its exponential $\exp(u)$ is a time stationary ordinary differential equation (ODE): $\partial p(t) / \partial t = u(t)$ and p is the image position. Then, the transformation s is updated by $\exp(u)$ as the form of $s \circ \exp(u)$. Based on this improvement,

the registration method can provide both efficient computations and invertible transformations between two geometries.

After the geometric registration, the next step is to relocate and reorient DTI fiber orientations of the template heart to the target heart as the final results based on the deformation field [24, 25].

2.4 Evaluations

Quantitative evaluation of the method is conducted by comparing the processed image with the corresponding reference image [12, 26–32]. The Dice similarity coefficient (DSC) is used as the performance assessment score of the similarity between both the reference and registered images [10–14,33]. Another evaluation method is the target registration error, which calculates the distance between corresponding markers in both images. We used the papillary muscles in the hearts as the anatomic markers for the calculation of the target errors. The distance between the mass centers in the corresponding markers was calculated for registration evaluation.

In order to evaluate the extracted cardiac fiber orientations from a template heart, the corresponding *ex vivo* DTI data of the same heart is utilized as the gold standard, which is mapped to the in vivo ultrasound geometry. Both estimated orientation and the gold standard from DTI at the same voxels are compared using two parameters: the acute angle error (AAE) and the inclination angle error (IAE). The acute angle is utilized to measure the angular separation between both orientations of the same fiber by inverting the absolute of their dot product in 3D into angles. But this angle is not sufficient enough for the evaluation because the cardiac fibers are arranged along the laminar sheets in myocardium rather than any direction. Thus, it will lead to more errors into the cardiac fiber estimations if only considering the acute angle. The inclination angle error serves as another parameter for the evaluation of fiber orientations [8].

3. RESULTS

3.1 Reconstruction of cardiac geometry from *in vivo* 3D ultrasound

First, the end of diastolic volume is reconstructed as shown in Figure 2(a) and its corresponding reconstructed 3D geometry of the heart after segmentation is shown in Figure 2(b).

Then, the cardiac geometries were compared between both *in vivo* ultrasound geometry and *ex vivo* MRI geometry of the same heart, shown in Figure 3. After deformable registration, the DSC between both geometries was 89.3%, which means that the geometry acquired from 3D ultrasound *in vivo* has a high similarity to that in the *ex vivo*, high-resolution MRI.

3.2 Accuracy of wrapping cardiac fiber orientations to the cardiac geometry of the 3D ultrasound *in vivo*

After the geometry reconstruction of *in vivo* 3D ultrasound, the DTI fiber orientations from a template heart were wrapped to the *in vivo* ultrasound geometry following the procedure in

Figure 1. The accuracy of the fiber orientation wrapping was validated by the cardiac fiber orientations of the target heart imaged by MR-DTI *ex vivo*.

As an illustration, cardiac fiber orientations were mapped from a template heart with MR-DTI data *ex vivo* to the geometry acquired from the *in vivo* 3D ultrasound images of another rat heart. The cardiac geometry in the diastole phase was segmented and reconstructed from the ultrasound volume. Finally, the fiber orientations were estimated by the proposed method, which used another *ex vivo* heart as the template. These results demonstrated the feasibility of estimating cardiac fiber orientations from the ultrasound images of the rat heart *in vivo*.

Moreover, the geometry registration accuracies between the target ultrasound geometry and the template MR-DTI geometry are listed in Table 1. Both AAE and IAE evaluations of the fiber wrapping accuracy are listed in the table.

4. DISCUSSION AND CONCLUSION

An imaging approach is proposed to acquire 3D ultrasound image volumes of the rat hearts *in vivo*. After image acquisition, its segmented cardiac myocardium is reconstructed as 3D geometry. Based on the *in vivo* 3D geometry, the accuracy of the cardiac fiber orientation wrapping from a different heart is validated by the diffusion tensor imaging data of *ex vivo* hearts. Both geometry and wrapped fiber orientation comparisons between *in vivo* and *ex vivo* data indicated that this approach could be applied in the research of the cardiac fiber orientations. Moreover, we also tested the feasibility of imaging beating hearts in vivo after an open-chest surgical procedure. This could provide an alternative method to *in vivo* assess the 3D geometry of the heart in the small animals.

ACKNOWLEDGEMENT

This research is supported in part by NIH grants R21CA176684, R01CA156775 and P50CA128301, Georgia Cancer Coalition Distinguished Clinicians and Scientists Award, and the Center for Systems Imaging (CSI) of Emory University School of Medicine.

REFERENCES

[1]. Qin X, Cong Z, Halig LV, Fei BW. Automatic Segmentation of Right Ventricle on Ultrasound Images Using Sparse Matrix Transform and Level Set. Proc SPIE. 2013; 8669:86690Q.

[2]. Qin X, Fei BW. Measuring myofiber orientations from high-frequency ultrasound images using multiscale decompositions. Phys Med Biol. 2014; 59(14):3907–3924. [PubMed: 24957945]

[3]. Lombaert H, Peyrat JM, Croisille P, et al. Human atlas of the cardiac fiber architecture: study on a healthy population. IEEE Trans Med Imaging. 2012; 31(7):1436–47. [PubMed: 22481815]

[4]. Sermesant M, Chabiniok R, Chinchapatnam P, et al. Patient-specific electromechanical models of the heart for the prediction of pacing acute effects in CRT: a preliminary clinical validation. Med Image Anal. 2012; 16(1):201–15. [PubMed: 21920797]

[5]. Vadakkumpadan F, Arevalo H, Ceritoglu C, et al. Image-based estimation of ventricular fiber orientations for personalized modeling of cardiac electrophysiology. IEEE Trans Med Imaging. 2012; 31(5):1051–60. [PubMed: 22271833]

[6]. Dawson D, Lygate CA, Saunders J, et al. Quantitative 3-dimensional echocardiography for accurate and rapid cardiac phenotype characterization in mice. Circulation. 2004; 110(12):1632–1637. [PubMed: 15364813]

[7]. Ram R, Mickelsen DM, Theodoropoulos C, et al. New approaches in small animal echocardiography: imaging the sounds of silence. Am J Physiol Heart Circ Physiol. 2011; 301(5):H1765–80. [PubMed: 21873501]

[8]. Qin X, Wang S, Shen M, Zhang X, Wagner MB, Fei BW. Mapping Cardiac Fiber Orientations from High-Resolution DTI to High-Frequency 3D Ultrasound. Proc SPIE. 2014; 9036:90361O.

[9]. Hari Sundar S, H. Shen DG, Biros G, et al. Estimating myocardial fiber orientations by template warping. 2006 3rd Ieee International Symposium on Biomedical Imaging: Macro to Nano. 2006; 1–3:73–76.

[10]. Akbari H, Fei BW. 3D ultrasound image segmentation using wavelet support vector machines. Medical Physics. 2012; 39(6):2972–2984. [PubMed: 22755682]

[11]. Fei BW, Yang X, Nye JA, et al. MR/PET quantification tools: Registration, segmentation, classification, and MR-based attenuation correction. Med Phys. 2012; 39(10):6443–54. [PubMed: 23039679]

[12]. Lv, G.; Yan, G.; Wang, Z. Bleeding detection in wireless capsule endoscopy images based on color invariants and spatial pyramids using support vector machines. Conf Proc IEEE Eng Med Biol Soc; 2011. p. 6643-6646.

[13]. Qin X, Lu G, Sechopoulos I, Fei BW. Breast Tissue Classification in Digital Tomosynthesis Images Based on Global Gradient Minimization and Texture Features. Proc SPIE. 2014; 9034:90341V.

[14]. Qin X, Wang S, Wan M. Improving reliability and accuracy of vibration parameters of vocal folds based on high-speed video and electroglottography. IEEE Trans Biomed Eng. 2009; 56(6): 1744–54. [PubMed: 19272979]

[15]. Fei BW, Duerk JL, Boll DT, et al. Slice-to-volume registration and its potential application to interventional MRI-guided radio-frequency thermal ablation of prostate cancer. IEEE Trans Med Imaging. 2003; 22(4):515–25. [PubMed: 12774897]

[16]. Fei BW, Duerk JL, Sodee DB, et al. Semiautomatic nonrigid registration for the prostate and pelvic MR volumes. Acad Radiol. 2005; 12(7):815–24. [PubMed: 16039535]

[17]. Fei BW, Duerk JL, Wilson DL. Automatic 3D registration for interventional MRI-guided treatment of prostate cancer. Comput Aided Surg. 2002; 7(5):257–67. [PubMed: 12582978]

[18]. Fei BW, Kemper C, Wilson DL. A comparative study of warping and rigid body registration for the prostate and pelvic MR volumes. Comput Med Imaging Graph. 2003; 27(4):267–81. [PubMed: 12631511]

[19]. Fei BW, Schuster D, Master V, et al. Incorporating PET/CT Images Into 3D Ultrasound-Guided Biopsy of the Prostate. Medical Physics. 2012; 39(6):3888–3888.

[20]. Fei BW, Wang H, Muzic RF Jr. et al. Deformable and rigid registration of MRI and microPET images for photodynamic therapy of cancer in mice. Med Phys. 2006; 33(3):753–60. [PubMed: 16878577]

[21]. Fei BW, Wheaton A, Lee Z, et al. Automatic MR volume registration and its evaluation for the pelvis and prostate. Phys Med Biol. 2002; 47(5):823–38. [PubMed: 11931473]

[22]. Lu G, Halig LV, Wang D, Chen ZG, Fei BW. Hyperspectral Imaging for Cancer Surgical Margin Delineation: Registration of Hyperspectral and Histological Images. Proc SPIE. 2014; 9036:90360S.

[23]. Wang HS, Fei BW. Nonrigid point registration for 2D curves and 3D surfaces and its various applications. Physics in Medicine and Biology. 2013; 58(12):4315–4330. [PubMed: 23732538]

[24]. Alexander DC, Pierpaoli C, Basser PJ, et al. Spatial transformations of diffusion tensor magnetic resonance images. Ieee Transactions on Medical Imaging. 2001; 20(11):1131–1139. [PubMed: 11700739]

[25]. Peyrat JM, Sermesant M, Pennec X, et al. A computational framework for the statistical analysis of cardiac diffusion tensors: application to a small database of canine hearts. IEEE Trans Med Imaging. 2007; 26(11):1500–14. [PubMed: 18041265]

[26]. Fei BW, Schuster DM, Master V, et al. A Molecular Image-directed, 3D Ultrasound-guided Biopsy System for the Prostate. Proc SPIE. 2012; 8316:831613.

[27]. Fei BW, Yang XF, Nye JA, et al. MR/PET quantification tools: Registration, segmentation, classification, and MR-based attenuation correction. Med Phys. 2012; 39(10):6443–6454. [PubMed: 23039679]

[28]. Yang X, Wu S, Sechopoulos I, Fei B. Cupping artifact correction and automated classification for high-resolution dedicated breast CT images. Med Phys. 2012; 39(10):6397–406. [PubMed: 23039675]

[29]. Lu G, Halig LV, Wang D, Chen GZ, Fei BW. Spectral-Spatial Classification Using Tensor Modeling for Cancer Detection with Hyperspectral Imaging. Proc SPIE. 2014; 9034:903413.

[30]. Lu GL, Halig LM, Wang DS, Chen GZ, Fei BW. Spectral-spatial classification for noninvasive cancer detection using hyperspectral imaging. Journal of Biomedical Optics. 2014; 19(10)

[31]. Sechopoulos I, Bliznakova K, Qin X, Fei BW, Feng SS. Characterization of the homogeneous tissue mixture approximation in breast imaging dosimetry. Med Phys. 2012; 39(8):5050–9. [PubMed: 22894430]

[32]. Qin X, Wu L, Jiang H, et al. Measuring body-cover vibration of vocal folds based on high frame rate ultrasonic imaging and high-speed video. IEEE Trans Biomed Eng. 2011; 58(8)

[33]. Qin X, Cong Z, Fei BW. Automatic segmentation of right ventricular ultrasound images using sparse matrix transform and level set. Physics in Medicine and Biology. 2013; 58(21):7609–24. [PubMed: 24107618]

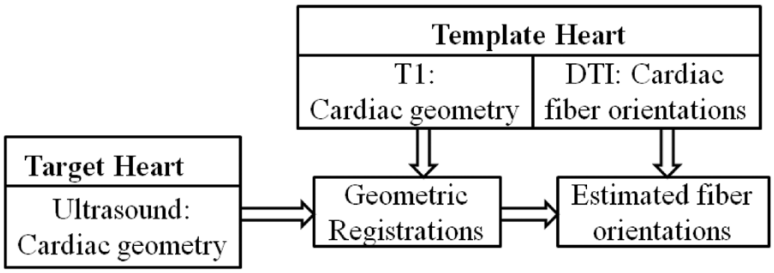

Figure 1.
Flowchart of wrapping cardiac fiber orientation from DTI to 3D ultrasound *in vivo*.

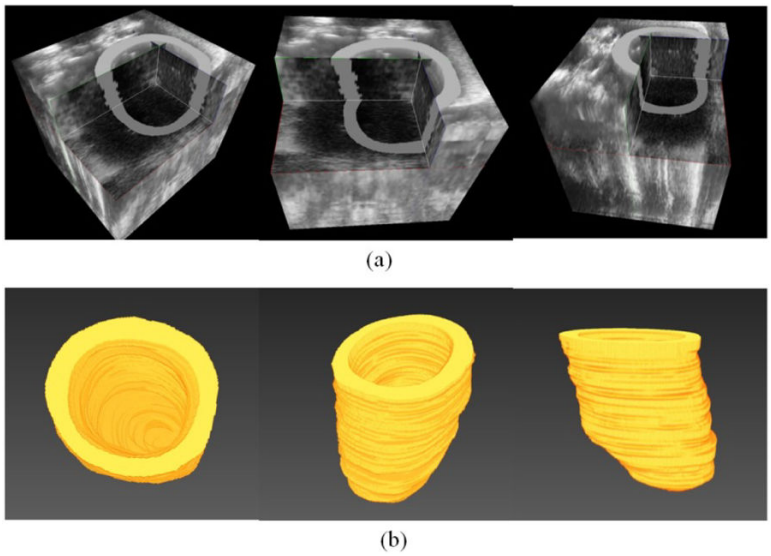

Figure 2.
Reconstructed ultrasound volume and the segmented heart geometry. (a) Ultrasound volume in the end of the diastole phase. (b) Segmented and reconstructed 3D geometry of the heart.

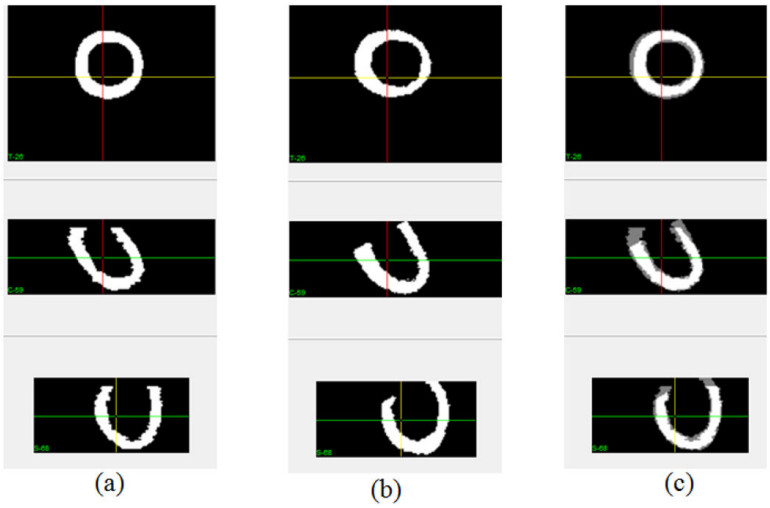

Figure 3.
Comparison between *in vivo* geometry and *ex vivo* geometry of the same heart. (a) *In vivo* geometry from 3D ultrasound. (b) *Ex vivo* geometry from MRI. (c) Comparison after rigid registration.

Table 1

Evaluation of the of the cardiac fiber orientations wrapping to the cardiac geometry of ultrasound *in vivo*

Target	Template	DSC (%)		AAE (degree)		IAE (degree)	
		Affine	Deform	Affine	Deform	Affine	Deform
In vivo ultrasound	*Ex vivo* DTI	71.6	89.3	32.5	24.7	26.3	22.4